Journal of Otology 18 (2023) 230–234

Contents lists available at ScienceDirect

Journal of Otology

journal homepage: www.journals.elsevier.com/journal-of-otology/

An evidenced-based diagnostic tool for superior semicircular canal dehiscence syndrome

Christian G. Fritz [a, b, *], Garrett G. Casale [a], Lulia A. Kana [a, c], Robert S. Hong [a, c]

[a] Michigan Ear Institute, Farmington Hills, Michigan, USA
[b] Department of Otorhinolaryngology–Head & Neck Surgery, University of Pennsylvania, Philadelphia, PA, USA
[c] Department of Otolaryngology–Head and Neck Surgery, Wayne State University, Detroit, MI, USA

ARTICLE INFO

Article history:
Received 2 August 2023
Accepted 20 September 2023

Keywords:
Clinical predictors
Diagnostic tool
SSCD
Superior semicircular canal dehiscence
Third window

ABSTRACT

Purpose: To construct a symptoms-based prediction tool to assess the likelihood of superior canal dehiscence (SSCD) on high-resolution CT.
Materials and methods: Mathematical modeling was employed to predict radiologic evidence of SSCD at a tertiary neurotology referral center.
Results: A total of 168 patients were included, of which 118 had imaging-confirmed SSCD. On univariate analysis significant predictors of SSCD presence were: sound/pressure-induced vertigo ($p = 0.006$), disequilibrium ($p = 0.008$), hyperacusis ($p = 0.008$), and autophony ($p = 0.034$). Multivariate analysis enabled a 14-point symptom-weighted tool to be developed, wherein a score of ≥6 raised the suspicion of SSCD (≥70% likelihood of being present), $R^2 = 0.853$.
Conclusions: The likelihood of SSCD on CT scan can be determined with a high degree of certainty based on symptoms recorded at presentation. Using the evidenced-based diagnostic tool validated herein, a score ≥6 with any symptom combination justifies ordering a CT scan.

1. Introduction

Superior semicircular canal dehiscence (SSCD) is caused by a thinning or absence of the bone overlying the superior semicircular canal (Minor et al., 1998; Kontorinis and Lenarz, 2022). The area of dehiscence is believed to cause a "third window" which results in a loss in the conduction of mechanical energy through the labyrinth upon sound and pressure stimulation (Kontorinis and Lenarz, 2022). Initially described by Minor et al. (1998), SSCD can lead to a variety of otologic and vestibular symptoms including disequilibrium, autophony, hyperacusis, aural fullness, hearing loss, tinnitus, and vertigo (Kontorinis and Lenarz, 2022; Naert et al., 2018).

A diagnosis of SSCD is based on patient symptoms in the setting of appropriate imaging and electrophysiologic testing results. Commonly used studies in the diagnosis of SSCD include a standard audiogram, high resolution CT (HRCT) of the temporal bone, and electrophysiologic testing such as vestibular myogenic evoked potentials (VEMPs), which may include both ocular VEMPs (oVEMPs) and cervical VEMPs (cVEMPs) (Kontorinis and Lenarz, 2022). However, several presenting symptoms of SSCD are quite non-specific when viewed in isolation, which can result in imprecise ordering of HRCT temporal bone scans. For this reason, many patients with a clinical suspicion for SSCD who undergo HRCT temporal bone yield negative results, increasing healthcare costs and exposure to ionizing radiation (Benamira et al., 2014).

Published evidence has identified factors that may be predictive of a diagnosis of SSCD, including cochlear symptoms (Benamira et al., 2014), decreased thresholds on cVEMP (Kim et al., 2022), increased oVEMP amplitudes (Zhang et al., 2021), and low frequency CHL (Zhang et al., 2021). While such clinical factors may be used to verify suspicion for SSCD independently, it again remains challenging to interpret in practice as patients often present with a quite varied combination of symptoms and objective findings (Naert et al., 2018; Zhou et al., 2007). To our knowledge, no

* Corresponding author. University of Pennsylvania Department of Otorhinolaryngology – Head and Neck Surgery, 800 Walnut Street, 18th Floor, Philadelphia, PA, 19107, USA.
E-mail address: christian.fritz@pennmedicine.upenn.edu (C.G. Fritz).

Peer review under responsibility of PLA General Hospital Department of Otolaryngology Head and Neck Surgery.

https://doi.org/10.1016/j.joto.2023.09.006

diagnostic tool exists to assist otolaryngologists in predicting a patient's overall probability of identifying SSCD radiographically in the setting of clinical suspicion for SSCD.

Herein, we propose a simple, accessible, and statistically-derived tool that predicts the likelihood of identifying the presence of radiographic SSCD based on an aggregate score of otologic and vestibular symptoms. We believe that faithful implementation of this model could be instrumental in guiding responsible ordering of HRCT temporal bone scans in the setting of clinical suspicion for SSCD.

2. Materials and methods

2.1. Subjects

A case series with chart review was performed in June 2023 to capture patients presenting with concern for SSCD between 2020 and 2021. ICD-10 codes used were H838X (other specified diseases of inner ear) and those with a specific diagnoses of possible superior canal dehiscence were identified from this patient dataset. Two hundred and fifty-three patients who presented to our tertiary neurotology referral center in the specified timeframe were identified. Charts with documented demographics, symptoms, and CT imaging data were included for analysis. History of prior ear surgery, audiometry, and performance on VEMP testing were collected. Institutional Review Board (IRB) approval was obtained (IRB #1826428-1).

2.2. Symptomatology

Signs and symptoms were extracted from patient charts. Auditory complaints were collected, including subjective hearing loss, hyperacusis, autophony, pulsatile tinnitus, non-pulsatile tinnitus, and ear fullness. Vestibular symptoms were also collected, including disequilibrium, positional vertigo, and pressure- or sound-induced vertigo. Symptom laterality (left, right, bilateral, or unknown) was noted. Patients with bilateral SSCD symptoms were excluded. Patients without imaging data were excluded.

2.3. Radiographic assessment

Imaging data was assessed via multiplanar reconstruction in the plane of Stenvers (perpendicular to the plane of the SSC) and the Pöschl projection (parallel to SSC). Scans were reviewed by both the neuro-radiologist and treating neurotologist. Patients missing the roof of the superior semicircular canal were classified as having “true” dehiscence. Patients with a “near” dehiscence demonstrating intact but thinned bone overlying the superior canal were excluded.

2.4. Objective testing

Standard audiograms were reviewed for each patient. Pure tone average, speech reception threshold, and word recognition score were recorded. Thresholds at 250 Hz were also recorded when available. VEMP testing was recorded when available, with both cVEMP thresholds and oVEMP amplitudes being recorded.

2.5. Data analysis and score development

Statistical analyses were performed using SPSS (version 24, IBM). Patients were split into two groups on the basis of CT imaging findings: SSCD present or SSCD absent. A univariate binary logistic analysis was performed to identify signs/symptoms associated with the presence of SSCD. To account for interaction between variables, a backward stepwise multivariate logistic regression analyses was employed, which was consistent with the prior literature (Minor et al., 1998; Wong et al., 2004). A final predictive model was constructed using factors found to be independently predictive of SSCD presence on multivariate analysis. Odds Ratio (OR) values represented the exponentiation of the B regression coefficient. Positive OR values were rounded to the closest integers to yield weighted score values, such that a higher numerical score for any given symptom portends a higher relative likelihood of SSCD presence on HRCT imaging. Scores for each variable were then combined to generate the Superior Semicircular Canal Dehiscence Symptom Inventory Assessment Tool (SSCD-SIAT). No score was awarded to variables with an OR below 1, which would represent a reduced likelihood of having the outcome of SSCD present on CT. Score summation for each symptom is not affected by the spcific combination of symptoms present. The maximum score allowed by the inventory was 14.

Non-parametric χ^2 tests were used to explore differences in symptom prevalence between groups. Fisher's exact test was applied for comparisons among small sample sizes. A receiver operating characteristic (ROC) curve analysis was generated to evaluate the diagnostic utility of the SSCD-SIAT tool. This plot represented test sensitivity versus 1-Specifity. The area under the curve (AUC) was used as a measure of diagnostic accuracy of the of SSCD-SIAT tool.

3. Results and analysis

3.1. Patient demographics

A total of 168 patients were included (average age: 49.3, range: 16–77; 42 male, 56 female).

Patients were divided into two groups based on imaging confirmed SSCD presence (n = 118) or SSCD absence (n = 50). Baseline characteristics by group are presented in Table 1.

3.2. Patient symptoms/objective testing

Signs/symptoms that were significantly more common in the symptomatic ear of patients with radiologically present SSCD included: abnormal oVEMP amplitudes >17 μV (49.2% vs 0%, $p = 0.026$); abnormal cVEMP thresholds ≤65 dB nHL (38.5% vs 0%, $p = 0.045$); disequilibrium (64.4% vs 42.0%, $p = 0.007$); hyperacusis (44.1% vs 22.0%, $p = 0.007$); sound/pressure-induced vertigo (28.8% vs 8.0%, $p = 0.003$); and autophony (45.8% vs 28.0%, $p = 0.032$) (Fig. 1). Although not statistically significant, low frequency (250Hz) bone conduction (BC) hyperacusis (supranormal hearing level) was more common among patients without SSCD ($\chi 2 = 2.3$, $p = 0.304$; Fishers Exact Test).

3.3. Mathematical modeling for diagnostic tool development

Symptomatology data was used to perform a univariate and multivariate logistic regression analysis (Table 2). On univariate analysis several significant predictors of SSCD presence were identified, including sound/pressure-induced vertigo ($p = 0.006$), disequilibrium ($p = 0.008$), hyperacusis ($p = 0.008$), and autophony ($p = 0.034$). Disequilibrium was most significant predictor of SSCD presence on multivariate analysis (OR = 2.508, $p = 0.020$). Variables with positive ORs on multivariate analysis indicated utility in predicting SSCD presence and were used to construct the 14-point SSCD-SIAT tool (Table 3). A binary logistic regression for VEMP data was performed on patients who underwent VEMP testing. Owing to the lack of VEMP data on SSCD negative patients, no significant VEMP-based predictors were identified (abnormal ipsilateral

Table 1
Baseline characteristics.

	All patients (n = 168)	SSCD present (n = 118)	SSCD absent (n = 50)
Sex [Female, n (%)]	105 (62.5)	74 (62.7)	31 (62.0)
Mean Age (SD)	52.4 (14.4)	53.1 (13.1)	50.6 (17.1)
Symptom laterality [Left, n (%)]	88 (52.3)	65 (55.1)	23 (46.0)
Prior ipsilateral ear surgery, n (%)	33 (19.6)	24 (20.3)	9 (18.0)
Pure tone average (4-tone), mean (SD)	21.7 (14.5)	21.5 (13.8)	22.1 (16.3)
Air Bone Gap (4-tone), mean (SD)	7.51 (7.6)	7.8 (7.8)	6.9 (7.2)
Air Bone Gap at 250Hz, mean (SD)	16.4 (15.0)	17.8 (15.0)	13.2 (14.5)
Speech recognition threshold (dB), mean (SD)	19.3 (14.3)	19.3 (13.3)	19.5 (16.4)
Word recognition score (%), mean (SD)	96.3 (12.1)	96.7 (10.2)	95.4 (15.7)

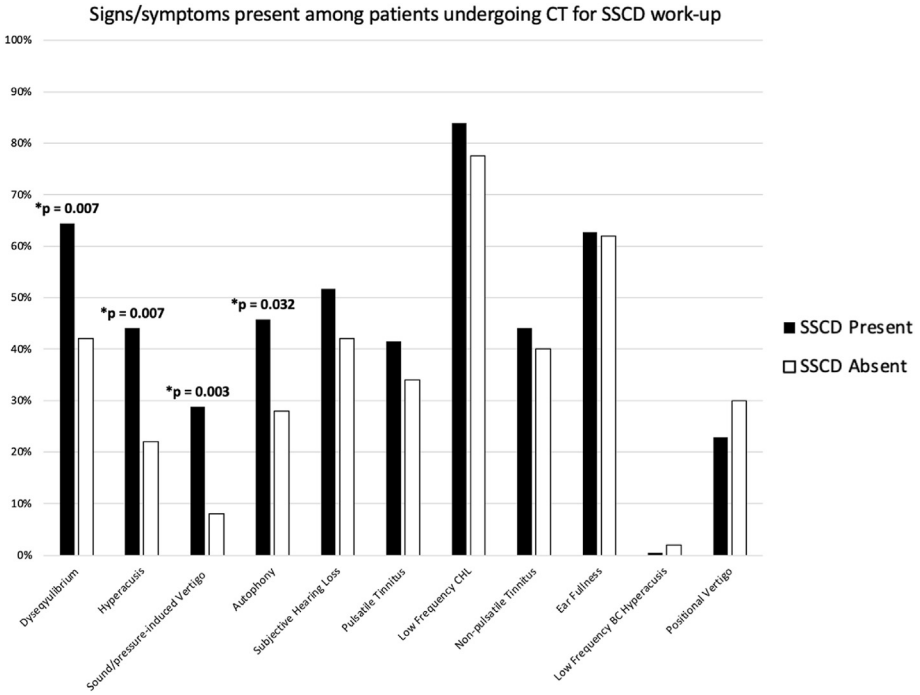

Fig. 1. Percentage of the patients with each sign/symptom stratified by SSCD presence. Variables were ordered in decreasing magnitude of difference between groups. Laterality of VEMP and audiogram data corresponds to symptomatic ear. Significant chi-square *p* values are shown ($p \leq 0.05$). (SSCD, Superior Semicircular Canal Dehiscence; VEMP, vestibular evoked myogenic potential).

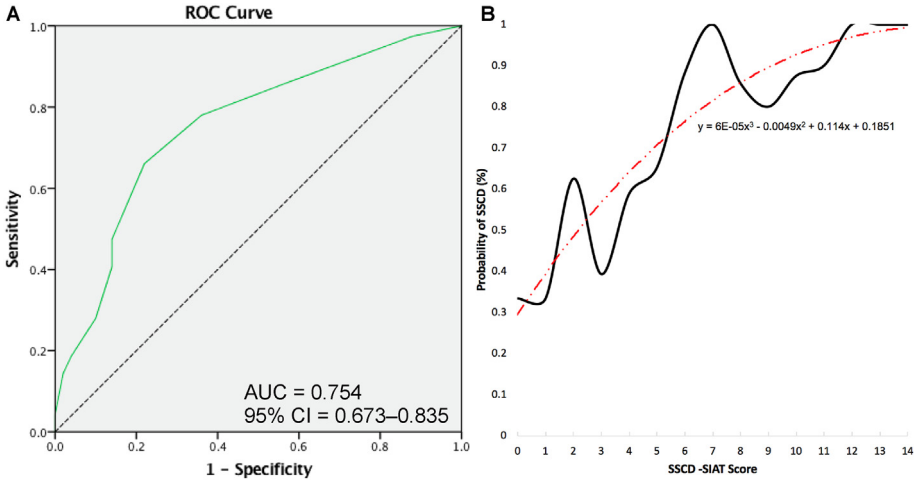

Fig. 2. A) ROC curve for accuracy of the SSCD-SIAT score in predicting presence of SSCD on CT imaging. Dashed diagonal reference line represents a sensitivity and specificity of zero. B) Probability of SSCD by SSCD-SIAT score. Black line circles represent observed frequency of SSCD among patients with a given SSCD-SIAT Score. Green polynomial line of best fit ($y = 5.74E\text{-}5x3 - 4.71E\text{-}3x2 + 0.1x + 0.29$) with $R^2 = 0.853$. Black vertical lines represent residual values. (ROC, Receiver operating characteristic; SSCD-SIAT, Superior Semicircular Canal Dehiscence - Symptom Identification Risk Indicator).

Table 2
Logistic regression analysis of signs/symptoms associated with SSCD presence.

Variable	Univariate Analysis				Multivariate Analysis			
	β	OR (Unadjusted)	95% CI for OR	*p*	β	OR (Unadjusted)	95% CI for OR	*p*
Sound/pressure induced vertigo	1.538	4.655	1.555-13.937	**0.006**	1.087	2.967	0.923-9.539	0.068
Dysequilibrium	0.916	2.499	1.271-4.914	**0.008**	0.920	2.508	1.155-5.447	**0.020**
Hyperacusis	1.027	2.793	1.304-5.982	**0.008**	0.823	2.277	0.988-5.245	0.053
Subjective hearing loss	0.391	1.478	0.758-2.881	0.252	0.700	2.013	0.946-4.283	0.069
Autophony	0.775	2.170	1.061-4.438	**0.034**	0.644	1.905	0.849-4.273	0.118
Pulsatile tinnitus	0.321	1.379	0.691-2.749	0.362	0.235	1.265	0.574-2.789	0.561
Non-pulsatile tinnitus	0.167	1.182	0.603-2.315	0.626	0.128	1.137	0.529-2.442	0.742
Ear fullness	0.030	1.031	0.521-2.039	0.931	−0.133	0.875	0.411-1.864	0.730
Positional vertigo	−0.368	0.692	0.330-1.454	0.331	−0.404	0.667	0.291-1.530	0.340

Table 3
Superior Semicircular Canal Dehiscence Symptom Inventory Assessment Tool (SSCD-SIAT) scoring guideline.

Variable	*p*	OR	Score
Sound/pressure induced vertigo	0.068	2.967	3
Dysequilibrium	0.020	2.508	3
Hyperacusis	0.053	2.277	2
Subjective hearing loss	0.069	2.013	2
Autophony	0.118	1.905	2
Pulsatile tinnitus	0.561	1.265	1
Non-pulsatile tinnitus	0.742	1.137	1
Total			14

*Final model constructed using variables found to be independently predictive of SSCD on multivariate analysis.

oVEMP, $p = 0.998$; abnormal ipsilateral cVEMP, $p = 0.998$).

The quantitative diagnostic accuracy of the SSCD-SIAT tool was assessed by measuring the Area Under the ROC curve (AUC). The AUC for this model was 0.814 (95% confidence interval, 0.742–0.886) (solid green line), which is within the AUC range of a clinically significant model (>0.750) (Fig. 2A). The probability of SSCD being present was plotted against SSCD-SIAT score. Probabilities were expressed as a percentage, which represented the percent of patients with that particular SSCD-SIAT score who had SSCD present (black line). A SSCD-SIAT score of ≥6 should raise the suspicion of SSCD (≥70% likelihood of being present), $R^2 = 0.853$ (Fig. 2B).

4. Discussion

Superior semicircular canal dehiscence can represent a diagnostic conundrum for both general otolaryngologists and neurotologists alike. The presenting symptoms can be quite varied and often inconsistent, greatly limiting the utility of a single symptom or objective finding towards establishing a diagnosis. Several symptoms have been associated with superior canal dehiscence including autophony, disequilibrium, hyperacusis, and tinnitus, among several others (Kontorinis and Lenarz, 2022; Naert et al., 2018).

The goal of this study was to construct a diagnostic tool based on patient symptoms at presentation that clinically predicts the presence of SSCD on imaging. We based our study design and concept off the Laboratory Risk Indicator for Necrotizing Fasciitis (LRINEC) study. The LRINEC scoring system is based on laboratory values that are used to predict the likelihood of necrotizing soft tissue infection. The authors of this prior study constructed a statistical model based on the odds ratios associated with clinical lab values as they relate to the presence of necrotizing fasciitis.

In our study, we (1) identified several presenting symptoms linked to the presence of SSCD and (2) constructed a predictive mathematical model using the associated odds ratios for each of the aforementioned variables. We identified sound/pressure induced vertigo, disequilibrium, hyperacusis, and autophony to be statistically associated with the presence of SSCD on multivariate regression. Interestingly, while pulsatile tinnitus and non-pulsatile tinnitus were not significantly associated with SSCD in this regression, we elected to include these variables in our model regardless given the preponderance of literature describing SSCD as a possible cause of tinnitus (Kontorinis and Lenarz, 2022; Naert et al., 2018; Ward et al., 2017). One explanation for the above discrepancy regarding tinnitus is the retrospective nature of the study. An inherent limitation of this study design is the inconsistent reporting of pulsatile tinnitus in clinical documentation. This may explain the lack of significance of pulsatile tinnitus as a predictive symptom for the radiologic presence of SSCD.

One feature of our mathematical model is that a score of zero corresponds to a non-zero value for predictive likelihood of SSCD on imaging. This stands to reason as this model is being used and constructed for use in a population in which there is a baseline non-zero clinical suspicion for superior canal dehiscence. Therefore, this feature of the model accurately reflects real-life clinical decision-making. Further, our model carries a high clinical specificity and sensitivity for the detection of SSCD, as evidenced by the strong AUC (0.814, 0.742–0.886).

It is well-reported in the literature that superior canal dehiscence on imaging does not necessarily imply the clinical presence of superior canal dehiscence syndrome. SSCD prevalence based on imaging or cadaveric studies vary across the literature, but it is clear that not all patients with SSCD on imaging manifest superior canal dehiscence syndrome (Masaki, 2011; Berning et al., 2019). We have minimized this potential discrepancy in our data by basing our model on signs and symptoms present in cases where superior semicircular canal dehiscence syndrome was suspected.

This report has several limitations. There was association between the presence of SSCD on imaging and low-frequency conductive hearing loss on audiogram in our regression models, an association that has been prior reported in the literature (Guan et al., 2020; Merchant and Rosowski, 2008). This may be due to inconsistent reporting of thresholds at 250 Hz in routine audiograms. Moreover, abnormalities in oVEMPs and cVEMPs in the setting of SSCD are well-described in the literature (Kim et al., 2022; Zuniga et al., 2013). Unfortunately, VEMP data was not collected in most patients without radiologic-confirmed superior canal dehiscence, which is an issue that has been raised in previous reports (Welgampola et al., 2008; Janky et al., 2013; Hunter et al., 2017; Roditi et al., 2009; Lin et al., 2019, 2021). This is likely explained by practice patterns in the ordering of VEMP testing (i.e. CT scans are ordered to confirm dehiscence prior to ordering VEMP testing). A future direction for our study would be to perform the same study prospectively using a standardized symptom inventory

to increase the consistency of documentation as it relates to presenting symptoms. Investigators could then apply the model presented in this study to the prospective population to assess goodness-of-fit.

5. Conclusion

This report describes a novel, symptoms-based tool that predicts the likelihood of SSCD on imaging. A score $\geq$6 with any symptom combination justifies ordering a CT scan for SSCD workup. This highly sensitive and specific model may help guide responsible ordering of CT scans in patients presenting with individually nondistinctive otologic complaints.

Financial disclosures

This research received no specific grant from any funding agency, commercial or not-for-profit sectors.

Informed consent

No experimentation with human subjects was conducted.

Declaration of competing interest

The authors declare none.

Acknowledgements

None.

References

Benamira, L.Z., Alzahrani, M., Saliba, I., 2014. Superior canal dehiscence: can we predict the diagnosis? Otol. Neurotol. 35, 338–343.

Berning, A.W., Arani, K., Branstetter 4th, B.F., 2019. Prevalence of superior semicircular canal dehiscence on high-resolution CT imaging in patients without vestibular or auditory abnormalities [published correction appears in *AJNR Am J neuroradiol*. 2019 jul;40(7):E39]. AJNR Am J Neuroradiol 40, 709–712.

Guan, X., Cheng, Y.S., Galaiya, D.J., Rosowski, J.J., Lee, D.J., Nakajima, H.H., 2020. Bone-conduction hyperacusis induced by superior canal dehiscence in human: the underlying mechanism. Sci. Rep. 10, 16564.

Hunter, J.B., Patel, N.S., O'Connell, B.P., et al., 2017. Cervical and ocular VEMP testing in diagnosing superior semicircular canal dehiscence. Otolaryngol. Head Neck Surg. 156, 917–923.

Janky, K.L., Nguyen, K.D., Welgampola, M., Zuniga, M.G., Carey, J.P., 2013. Air-conducted oVEMPs provide the best separation between intact and superior canal dehiscent labyrinths. Otol. Neurotol. 34, 127–134.

Kim, D.H., Kim, S.W., Kim, S.H., Jung, J.H., Hwang, S.H., 2022. Usefulness of cervical vestibular-evoked myogenic potentials for diagnosing patients with superior canal dehiscence syndrome: a meta-analysis. Otol. Neurotol. 43, 146–152.

Kontorinis, G., Lenarz, T., 2022. Superior semicircular canal dehiscence: a narrative review. J. Laryngol. Otol. 136, 284–292.

Lin, K., Lahey, R., Beckley, R., et al., 2019. Validating the utility of high frequency ocular vestibular evoked myogenic potential testing in the diagnosis of superior semicircular canal dehiscence. Otol. Neurotol. 40, 1353–1358.

Lin, K.F., Bojrab 2nd, D.I., Fritz, C.G., Vandieren, A., Babu, S.C., 2021. Hearing outcomes after surgical manipulation of the membranous labyrinth during superior semicircular canal dehiscence plugging or posterior semicircular canal occlusion. Otol. Neurotol. 42, 806–814.

Masaki, Y., 2011. The prevalence of superior canal dehiscence syndrome as assessed by temporal bone computed tomography imaging. Acta Otolaryngol. 131, 258–262.

Merchant, S.N., Rosowski, J.J., 2008. Conductive hearing loss caused by third-window lesions of the inner ear. Otol. Neurotol. 29, 282–289.

Minor, L.B., Solomon, D., Zinreich, J.S., Zee, D.S., 1998. Sound- and/or pressure-induced vertigo due to bone dehiscence of the superior semicircular canal. Arch. Otolaryngol. Head Neck Surg. 124, 249–258.

Naert, L., Van de Berg, R., Van de Heyning, P., et al., 2018. Aggregating the symptoms of superior semicircular canal dehiscence syndrome. Laryngoscope 128, 1932–1938.

Roditi, R.E., Eppsteiner, R.W., Sauter, T.B., Lee, D.J., 2009. Cervical vestibular evoked myogenic potentials (cVEMPs) in patients with superior canal dehiscence syndrome (SCDS). Otolaryngol. Head Neck Surg. 141, 24–28.

Ward, B.K., Carey, J.P., Minor, L.B., 2017. Superior canal dehiscence syndrome: lessons from the first 20 years. Front. Neurol. 8, 177.

Welgampola, M.S., Myrie, O.A., Minor, L.B., Carey, J.P., 2008. Vestibular-evoked myogenic potential thresholds normalize on plugging superior canal dehiscence. Neurology 70, 464–472.

Wong, C.H., Khin, L.W., Heng, K.S., Tan, K.C., Low, C.O., 2004. The LRINEC (Laboratory Risk Indicator for Necrotizing Fasciitis) score: a tool for distinguishing necrotizing fasciitis from other soft tissue infections. Crit. Care Med. 32, 1535–1541.

Zhang, L., Creighton Jr., F.X., Carey, J.P., 2021. A cohort study comparing importance of clinical factors in determining diagnosis and treatment for superior semicircular canal dehiscence syndrome. Otol. Neurotol. 42, 1429–1433.

Zhou, G., Gopen, Q., Poe, D.S., 2007. Clinical and diagnostic characterization of canal dehiscence syndrome: a great otologic mimicker. Otol. Neurotol. 28, 920–926.

Zuniga, M.G., Janky, K.L., Nguyen, K.D., Welgampola, M.S., Carey, J.P., 2013. Ocular versus cervical VEMPs in the diagnosis of superior semicircular canal dehiscence syndrome. Otol. Neurotol. 34, 121–126.